Improved mobility in InAlN/AlGaN two-dimensional electron gas heterostructures with an atomically smooth heterointerface

Daiki Hosomi[1]*, Yuta Miyachi[1], Takashi Egawa[1,2] and Makoto Miyoshi[1,2]

[1]*Research Center for Nano Device and System, Nagoya Institute of Technology, Nagoya 466-8555, Japan*

[2]*Innovation Center for Multi-Business of Nitride Semiconductors, Nagoya Institute of Technology, Nagoya 466-8555, Japan*

E-mail: d.hosomi.904@nitech.jp

We attempted to improve the mobility of InAlN/AlGaN two-dimensional electron gas (2DEG) heterostructures by achieving an atomically smooth heterointerface in metalorganic chemical vapor deposition processes. In the result, it was confirmed that the high-growth-rate AlGaN layer was very effective to improve the surface morphology. The atomically smooth surface morphology with a root-mean-square roughness of 0.26 nm was achieved for an $Al_{0.15}Ga_{0.85}N$ layer under the growth rate of approximately 6 μm/h. Furthermore, nearly lattice-matched $In_{0.17}Al_{0.83}N/Al_{0.15}Ga_{0.85}N$ 2DEG heterostructures with the atomically smooth heterointerface exhibited a 2DEG mobility of 242 cm^2/Vs with a 2DEG density of 2.6×10^{13} $/cm^2$, which was approximately 1.5 times larger than the mobility in a sample grown under original conditions.

1. Introduction

Heterostructure field-effect transistors (HFETs) based on AlGaN/GaN two-dimensional-electron gas (2DEG) structures have been viewed as a most promising candidate for next generation high-power/high-frequency electronic devices, owing to their high breakdown voltages, large 2DEG densities and high electron mobilities.[1-8] In addition to conventional AlGaN/GaN 2DEG heterostructures, AlGaN-channel heterostructures have also been attracting much attention because they exhibit excellent device characteristics such as higher breakdown voltages and less temperature dependence at high temperatures.[9-19] Nanjo *et al*. demonstrated AlGaN/AlGaN HFETs with extremely higher breakdown voltage compared to AlGaN/GaN HEMTs.[9,11] Hatano *et al*. reported that AlGaN-channel devices showed less temperature dependence in high-temperature device operations than that of conventional GaN-channel devices.[12,13] On the other hand, 2DEG heterostructures employing InAlN barrier layers instead of AlGaN barrier layers have also been widely studied for the past decade. This is because a large spontaneous polarization in lattice-matched InAlN/GaN heterostructures generates a large 2DEG density of over $2 \times 10^{13}/cm^2$ even without a piezoelectric polarization effect related to a large in-plane strain.[20,21] Indeed, several research groups have reported on InAlN-barrier HFETs with high 2DEG densities and excellent electrical properties.[22-25] Recently, we have reported the growth and characterization results about novel InAlN/AlGaN heterostructures and FETs, which were conducted aiming for a new high-power nitride platform.[26-28] Although we have confirmed that the potential of InAlN/AlGaN heterostructures, there were found to be a few issues to be solved for considering the practical use of InAlN/AlGaN HFETs.[28] One of the most important issues is concerning their 2DEG mobility. That is, the 2DEG mobility was measured to be less than 170 cm^2/Vs at highest, while the theoretical mobility limit exceeds

300 cm^2/Vs.[26,27] This was understood to be because the interface roughness scattering significantly suppressed the 2DEG mobility.[27] Recently, we have therefore studied on the improvement in the 2DEG mobility for InAlN/AlGaN heterostructures by achieving an atomically smooth heterointerface.[29] This paper presents our most recent research focusing on the material growth process and their microstructure analyses.

2. Experimental

Samples were grown in a horizontal metalorganic chemical vapor deposition (MOCVD) system (Taiyo Nippon Sanso SR2000), where trimethyl gallium, trimethyl aluminum, and trimethyl indium were used as group-III sources, and NH_3 was used as a group-V source. A 2-in-diameter AlN/sapphire template (AlN template), which had a 1-μm-thick epitaxial AlN film on a *c*-face sapphire, was used as an underlying substrate. The typical X-ray rocking curve (XRC) full widths at half maxima (FWHMs) for the epitaxial AlN film were approximately 100 s and 1,500 s for the (0002) and $(10\bar{1}2)$ reflections, respectively. Fig. 1 shows schematic of a GaN-free InAlN/AlGaN heterostructure employed in this study. The heterostructure consisted of, from bottom to top, a 2-μm-thick AlGaN channel layer, a 1-nm-thick AlN inter-layer, and a 15-nm-thick InAlN barrier layer. The 1-nm-thick AlN interfacial layer was employed not only for enhancing 2DEG carrier confinement in the channel, but also for protecting the AlGaN surface during the growth interval. The InAlN barrier layer was grown to be lattice-matched to the underlying AlGaN channel layers.[26] In this study, in order to improve the InAlN/AlGaN heterointerface quality, we introduced two different concepts as experimental factors in accordance with the results reported by Hirayama *et al*.[30] One is an idea of a regrown AlN layer, which was inserted prior to the growth of AlGaN channel layer for reducing the cracks

and/or threading dislocations. The regrown AlN layer contains a few different-growth-rate AlN layers as shown in Fig. 1. The other is an idea concerning the growth rate of the AlGaN-channel layer, in which high growth rates up to approximately 6 μm/h, three times higher than that in our previous work, were examined.[26,27] The surface morphology for the MOCVD-grown samples was observed by atomic force microscopy (AFM). To analyze the surfaces of the channel AlGaN and regrown AlN layers, additional samples without overlying layers were prepared. The layer thicknesses were estimated from the growth rate, and the compositions of the heterostructure samples were confirmed using X-ray diffraction (XRD) measurements. The cross-sectional microstructures were observed by transmission electron microscopy (TEM). The depth profiling of the 2DEGs was evaluated using a capacitance-voltage ($C-V$) measurement system (Nanometrics, ECVpro^{TM}), while the 2DEG densities and mobilities were determined using the Hall effect measurement.

3. Results and discussion

First, this study began with the simultaneous introduction of the two concepts, the regrown AlN layer and the high-growth-rate AlGaN layer. Fig. 2(a) shows a surface AFM image for an AlGaN layer grown on the regrown AlN layer with a high growth rate of approximately 6 μm/h. For comparison, Fig. 2(b) shows the result of a sample grown under the original growth conditions. Here, the sample seen in Fig. 2(b) is the same as that shown in our previous study.[26] As is obvious in comparison between the two images, the sample grown under the modified conditions exhibited a much smoother surface morphology with clear atomic steps, compared to the sample grown under the original conditions. The measured root-mean-square (RMS) roughness was confirmed to be significantly reduced from 1.2 nm to 0.26 nm. Thus, we conclude that the growth conditions applied to this study

were surely effective to the improve the AlGaN surface morphology.

In order to investigate the effect of the regrown AlN layer on the improvement of AlGaN surface morphology in more detail, AFM and cross-sectional TEM observations were then carried out. Figs. 3(a) and 3(b) show cross-sectional bright-field scanning TEM images for MOCVD-grown AlGaN/AlN stacking structures, which correspond to the samples seen in Figs. 2(a) and 2(b), respectively. In these figures, surface AFM images for AlN layers without the growth of overlying AlGaN layers are also shown. That is, the AFM images seen in Figs. 2(a) and 2(b) show the surface morphologies for the regrown AlN layer and the epitaxial AlN layer of the AlN template, respectively. From the cross-sectional TEM images seen in Fig. 3, it was found that the threading dislocations in AlGaN layers considerably decreased compared to the underlying AlN layers. However, their cross-sectional microstructures including the threading dislocation propagation showed almost no distinctive difference between the two samples. On the other hand, surface AFM images for the AlN layers seen in Fig. 3 revealed that the regrown AlN layer has a rougher surface than that of the epitaxially-grown underlying AlN layer. Regarding this phenomenon, we considered two possibilities. One is that the rough AlN surface enhanced the inhomogeneous nucleation and caused the lateral overgrowth of AlGaN layer. The other is that the regrown AlN layer did not play a critical part for the improvement of AlGaN surface morphology just except the suppression of crack generation.

In order to separate the effects of the growth rate and the regrown AlN layer, we grew several AlGaN samples at various growth rates without the insertion of the regrown AlN layer, and analyzed their surface morphologies. Fig. 4(a) shows the relationship between the RMS roughness values obtained from the AFM analyses and the growth rates in the AlGaN layers, in which all samples were grown without the insertion of the regrown AlN layer. In these

figures, the surface AFM images for the respective AlGaN samples were also shown. As seen in this figure, AlGaN layers grown with high growth rates tend to show a clear step-flow growth mode, and exhibited atomically smooth surfaces with low RMS roughness values. In contrast, the sample grown with a low growth rate showed a considerably rough surface. Thus, we came to conclude that the improvement of the AlGaN surface morphology strongly depended on their growth rate. Even if the regrown AlN layer also contributed to the improvement of the AlGaN surface morphology, its effect would be much lower than the effect of the growth rate. This conclusion seems consistent with the previous results reported by Hirayama *et al*.[30] So far as we know, however, there has been almost no scientific explanation regarding the effect of the high-speed growth. More detailed and comprehensive study is necessary for sufficient understanding of this phenomenon.

On the basis of the above, we grew an $In_{0.17}Al_{0.83}N/Al_{0.15}Ga_{0.85}N$ 2DEG heterostructure as shown in Fig. 1 under the modified growth conditions, and characterized its 2DEG properties by *C*-*V* and Hall effect measurements. Fig. 5 shows a result of the *C*-*V* depth profiling, from which it was confirmed that electrons were highly concentrated around a depth of approximately 15 nm from the surface, which corresponds to the InAlN barrier thickness. This confirmed that the electrons were two-dimensionally generated at the InAlN/AlGaN heterointerface. Then, 2DEG density, 2DEG mobility and sheet resistance were measured to be 2.6×10^{13} /cm^2, 242 cm^2/Vs and 998 Ω/sq, respectively, by Hall effect measurement at room temperature. Fig. 6 compares the relationships between the measured 2DEG densities and mobilities for the InAlN/AlGaN heterostructures grown in this study and in our previous work.[27] As seen in this figure, the measured 2DEG mobility achieved to approximately 1.5 times higher than those measured in our past work. This is possibly attributed to the improved heterointerface. Fig. 7 shows the relationship between Al content

in AlGaN channel and the 2DEG mobilities, in which the theoretical mobility limit of AlGaN-channel 2DEG heterostructures[27] was also plotted. From this, it was confirmed that the measured 2DEG mobility is fairly closer to the theoretical limit than those for our previous work. As a result, the sheet resistance of InAlN/AlGaN heterostructures has come closer to those of conventional AlGaN/GaN heterostructures. This result should be accepted to be a positive thing because the specific on-resistance of the power electronic devices depends on not only their breakdown voltages but also the sheet resistance of epiwafers. [28]

4. Conclusions

We conducted the research for improving the 2DEG mobility in InAlN/AlGaN 2DEG heterostructures. It was confirmed that the high growth rates for the AlGaN layer strongly affected the improvement of the AlGaN surface morphology rather than the insertion of initial regrown AlN layer and thereby results in a high 2DEG mobility. An $In_{0.17}Al_{0.83}N/Al_{0.15}Ga_{0.85}N$ heterostructure with the high-growth-rate AlGaN layer showed an improved 2DEG mobility of 242 cm^2/Vs with a 2DEG density of 2.6×10^{13} $/cm^2$.

Acknowledgement

This work was partially supported by the Super Cluster Program of the Japan Science and Technology (JST) Agency and JSPS KAKENHI Grant Number JP16K06298.

References

1) J. W. Chung, W. E. Hoke, E. M. Chumbes, and T. Palacios, IEEE Electron Device Lett. **31**, 195 (2010).

2) T. Kikkawa, M. Kanamura, T. Ohki, K. Imanishi, K. Watanabe, and K. Joshin, ECS Trans. **50**, 323 (2013).

3) T. Egawa, IEEE International Electron Devices Meeting (IEDM) Tech. Dig., 2012, p. 27.1.1.

4) C. M. Jeon, J. H. Lee, J. H. Lee, and J. L. Lee, IEEE Electron, Device Lett. **25**, 120 (2004).

5) N. Ikeda, Y. Niiyama, H. Kambayashi, Y. Sato, T. Nomura, and S. Yoshida, Proc. IEEE **98**, 1151 (2010).

6) U. K. Mishra, P. Parikh, and Y. -F. Wu, Proc. IEEE **90**, 1022 (2002)

7) S. Selvaraj, A. Watanabe, A. Wakejima, and T. Egawa, IEEE Electron Device Lett. **33**, 1375 (2012).

8) S. Mase, T. Egawa, and A. Wakejima, Appl. Phys. Express **8**, 036601 (2015).

9) T. Nanjo, M. Takeuchi, M. Suita, Y. Abe, T. Oishi, Y. Tokuda, and Y. Aoyagi, IEEE International Electron Devices Meeting (IEDM) Tech. Dig., 2007, p. 397.

10) T. Nanjo, M. Takeuchi, M. Suita, T. Oishi, Y. Abe, Y. Tokuda, and Y. Aoyagi, Appl. Phys. Lett. **92**, 263502 (2008).

11) T. Nanjo, M. Takeuchi, M. Suita, Y. Abe, T. Oishi, Y. Tokuda, and Y. Aoyagi, Appl. Phys. Express **1**, 011101 (2008).

12) M. Hatano, N. Kunishio, H. Chikaoka, J. Yamazaki, Z. B. Makhzani, N. Yafune, K. Sakuno, S. Hashimoto, K. Akita, Y. Yamamoto, and M. Kuzuhara, IEEE International Conference on Compound Semiconductor Manufacturing Technology (CS MANTECH) Dig., 2010, p. 101.

13) M. Hatano, N. Yafune, H. Tokuda, Y. Yamamoto, S. Hashimoto, K. Akita, and M.

Kuzuhara, IEICE Trans, Electron. **E95-C**, 1332 (2012).

14) S. Hashimoto, K. Akita, T. Tanabe, H. Nakahata, K. Takeda, and H.Amano, Phys. Status Solidi C **7**, 1938 (2010).

15) S. Hashimoto, K. Akita, Y. Yamamoto, M. Ueno, T. Nakamura, N. Yafune, K. Sakuno, H. Tokuda, M. Kuzuhara, K. Takeda, M. Iwaya, and H. Amano, Phys. Status Solidi C **9**, 373 (2012).

16) C. M. Jeon, J. H. Lee, J. H. Lee, and J. L. Lee, IEEE Electron Device Lett. **25**, 120 (2004).

17) J. Liu, Y. Zhou, R. Chu, Y. Cai, K. J. Chen, and K. M. Lau, IEDM Tech. Dig., 2004, p. 811.

18) A. Raman, S. Dasgupta, S. Rajan, J. S. Speck, and U. K. Mishra, Jpn. J. Appl. Phys. **47**, 3359 (2008).

19) J. Liu, Y. Zhou, R. Chu, Y. Cai, K. J. Chen, and K. M. Lau, IEEE Electron Device Lett. **26**, 145 (2005).

20) J. Kuzmik, IEEE Electron Device Lett. **22**, 510 (2001).

21) M. Miyoshi, Y. Kuraoka, M. Tanaka, and T. Egawa, Appl. Phys. Express **1**, 081102 (2008).

22) J. J. Freedsman, A. Watanabe, T. Ito, and T. Egawa, Appl. Phys. Express **7**, 104101 (2014).

23) A. Watanabe, J. J. Freedsman, R. Oda, T. Ito, and T. Egawa, Appl. Phys. Express **7**, 041002 (2014).

24) H. Saito, Y. Takada, M. Kuraguchi, M. Yumoto, and K. Tsuda, Phys. Status Solidi C **10**, 824 (2013).

25) Q. Fareed, A. Tarakji, J. Dion, M. Islam, V. Adivarahan, and A. Khan, Phys. Status Solidi C **8**, 2454 (2011).

26) M. Miyoshi, S. Fujita, and T. Egawa, Appl. Phys. Express **8**, 021001 (2015).

27) M. Miyoshi, S. Fujita, and T. Egawa, Appl. Phys. Express **8**, 051003 (2015).

28) M. Miyoshi, T. Tsutsumi, G. Nishino, Y. Miyachi, M. Okada, J. J. Freedsman, and T.Egawa, J. Vac. Sci. Tech. B **34**, 050602 (2016).

29) D. Hosomi, Y. Miyachi, T. Egawa, and M. Miyoshi, Ext. Abstr. Solid State Devices and Materials, 2017, p. 635.

30) H. Hirayama, N. Maeda, S. Fujikawa, S. Tayoda, and N. Kamata, Jpn. J. Appl. Phys. **53**, 100209 (2014).

Figure captions

Figure 1. Schematic cross section of InAlN/AlGaN 2DEG heterostructure.

Figure 2. (Color online) Surface AFM images for the $Al_{0.15}Ga_{0.85}N$ layers grown under (a) the modified growth conditions and (b) the original growth conditions.

Figure 3. (Color online) Cross-sectional bright-field scanning TEM images for AlGaN/AlN stacking structures for samples grown under (a) modified growth conditions and (b) original growth conditions. Surface AFM images for AlN layers are also shown for the respective samples.

Figure 4. (Color online) Relationship between the RMS roughness values obtained from the AFM observations and the growth rates in the $Al_{0.15}Ga_{0.85}N$ layers, in which all samples were grown without the insertion of the regrown AlN layer. Surface AFM images for the corresponding AlGaN layers are also shown.

Figure 5. (Color online) *C*-*V* depth profiling of the $In_{0.17}Al_{0.83}N/Al_{0.15}Ga_{0.85}N$ heterostructure.

Figure 6. (Color online) Relationship between 2DEG densities and mobilities for the $In_{0.17}Al_{0.83}N/Al_{0.15}Ga_{0.85}N$ heterostructure measured by Hall effect measurements at room temperature. Dashed lines represent constant sheet resistance R_{sh} lines. Blue solid diamond dots our previous data.[26)]

Figure 7. (Color online) Relationship between Al contents in AlGaN channels and room-temperature 2DEG mobilities. Dashed line represents the calculated theoretical mobility limit at the 2DEG density of 2.5×10^{13} /cm^2. Blue solid diamond dots represent our previous data.[26)]

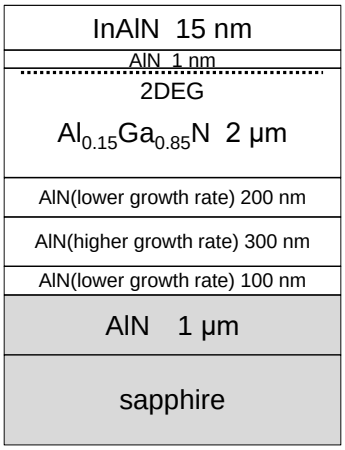
InAlN 15 nm
AlN 1 nm
2DEG
$Al_{0.15}Ga_{0.85}N$ 2 μm
AlN(lower growth rate) 200 nm
AlN(higher growth rate) 300 nm
AlN(lower growth rate) 100 nm
AlN 1 μm
sapphire

Figure 1

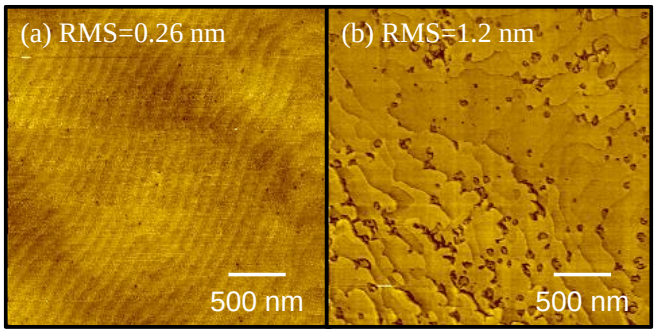

Figure 2

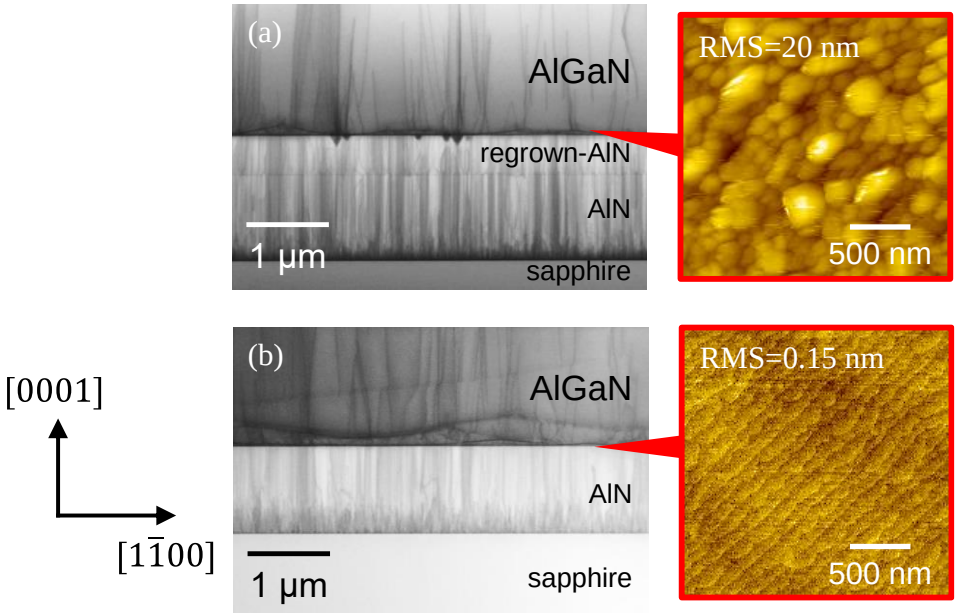
(a)
AlGaN
regrown-AlN
AlN
1 μm
sapphire
RMS=20 nm
500 nm
[0001]
[1$\bar{1}$00]
(b)
AlGaN
AlN
1 μm
sapphire
RMS=0.15 nm
500 nm

Figure 3

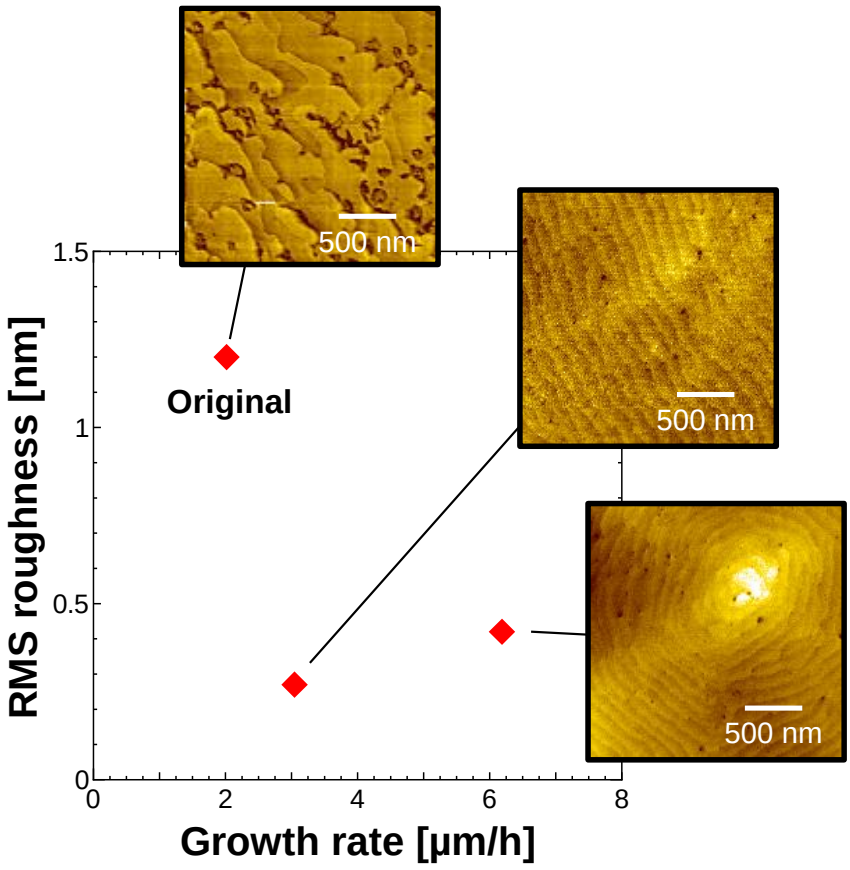
500 nm
Original
500 nm
500 nm
RMS roughness [nm]
Growth rate [μm/h]
0
0.5
1
1.5
0
2
4
6
8

Figure 4

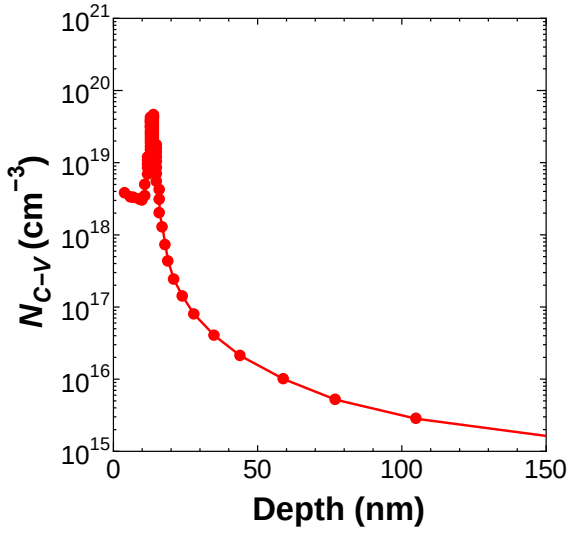
10^{21}
10^{20}
10^{19}
10^{18}
10^{17}
10^{16}
10^{15}
N_{C-V} (cm^{-3})
0
50
100
150
Depth (nm)

Figure 5

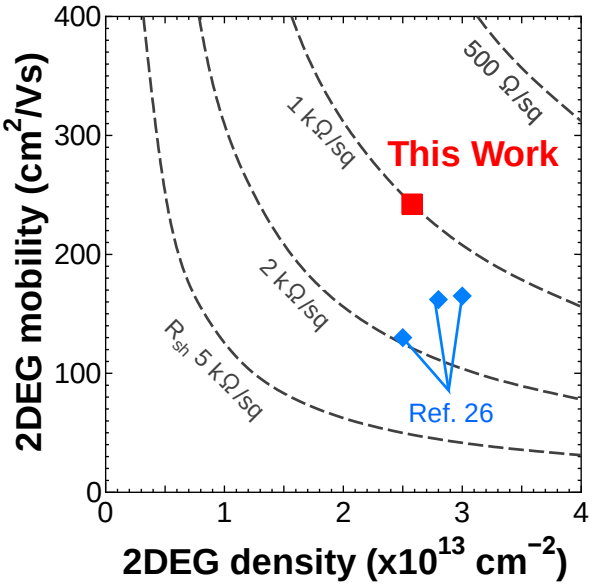
400
300
200
100
0
0
1
2
3
4
2DEG mobility (cm²/Vs)
2DEG density (x10¹³ cm⁻²)
500 Ω/sq
1 kΩ/sq
2 kΩ/sq
Rsh 5 kΩ/sq
This Work
Ref. 26

Figure 6

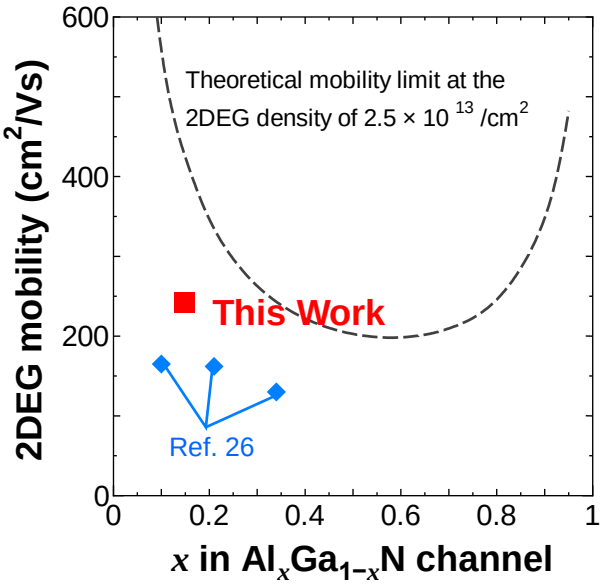
600
400
200
0
0
0.2
0.4
0.6
0.8
1
2DEG mobility (cm²/Vs)
x in AlxGa1−xN channel
Theoretical mobility limit at the
2DEG density of 2.5 × 10 13 /cm2
This Work
Ref. 26

Figure 7